International Journal of Environmental Sciences
ISSN: 2229-7359
Vol. 11 No. 23s, 2025
https://theaspd.com/index.php

Synthesis, Characterization, In Vitro Antioxidant Activity And In Silico Study On Potential Inhibitory Action Of Novel Curcumin Acquired Copper (II) Complexes Against COVID-19 Main Protease(M^{pro}:6LU7)

Richa Kothari
Department of Chemistry ITM University, Gwalior (M.P.)-474005 -India, richakothari@itmuniversity.ac.in

Abstract

A series of three novel curcumin acquired hydrazone Schiff base copper (II) coordination complexes were synthesized by template method using Curcumin, 2- hydrazine hydrazide and copper salts (copper chloride ,acetate and sulphate in 2:1 molar ratio. All synthesised derivatives have been characterized by elemental analysis, molar conductance ,thermogravimatric analysis , UV-Vis, FT-IR .On the basis of physico-chemical measurements the following empirical formula have been assigned to the copper (II) coordination compound $[Cu\ (H_2L)_2\ Cl_2].\ 2H_2O$, $[Cu\ (H_2L)_2\ (SO_4)_2].5H_2O$, $[Cu\ (H_2L)_2\ (CH_3\ COO)_2\ ]5H_2O$ *where* H_2L *is Hydrazone Schiff base ligand. Total antioxidant activity were tested via DPPH method and this antioxidant activity was appraise by comparison with standard substance like DPPH. The result of antioxidant activity showed that coordinate copper complexes are more influential antioxidant agents than curcurmin acquired hydrazone Schiff base ligand. Molecular docking studies were carried out to ascertain the inhibitory action of studied ligand and its copper (II) complex against the Main protease (6LU7) of novel coronavirus (COVID-19).The result of the docking of ligand and copper complex showed a significant inhibitory action against the Main protease (M^{pro}) of SARS-CoV-2 and the binding energy (ΔG) values of the ligand and coordinated complexes against the protein 6LU7 have found to be -8.7Kcal/mol & -9.5 Kcal/mol .*

Keywords: *Curcumin derivatives, Molecular docking, Antioxidant activity ,Sars- CoV -2 , 6LU7.*

INTRODUCTION

The coronavirus disease -19 (COVID-19) pandemic is still devasting the world causing significant social,economic and political chaos corresponding to the absence of globally approved antiviral drugs for treatment and vaccines for controlling the pandemic ,number of cases and /or mortalities are still rising .Current patient management relies on supportive treatment and the use of repurposed drugs as an indispensable option. Since emergence of corona virus in Wuhan, China[1] (Huang et al , 2020) COVID-19 caused by the novel ' SARS ' CoV-2 has been causing significant mortality and morbidity all over the world . The pandemic provoke global attention affecting every corner of the world and is changing the social , economic , and political status of the globe. Restrain the spread of the virus has been challenging because it has diversified means of transmission like direct contact , via droplets , airborne, fomite, fecal -oral , blood born, sexual intercourse , ocular, mother to child and animal to human[2] (Patel et al. 2020) .Although corona virus primarily cause a mild respiratory illness significant proportions of patients experience severe disease with outcomes of death .Moreover, there is also a significant number of asymptomatic infections that can transmit the virus to other . COVID-19 patients with underlying conditions are known to have a higher risk of developing a severe disease [3,4](Chow et al. 2020; Zhang et al., 2020c) .The primary treatment of COVID-19 relies on symptomatic and oxygen therapy to manage respiratory impairment. In the emergency case of complicated disease ,ICU is required because of acute respiratory distress syndrome (ARDS) or multiple organ failure (MOF)[5,6,7] (Cascella et al., 2020 a ; Chen et al.2020 a ; Gattinoni et al. , 2020). Fifteen drugs like chloroquine, hydroxychloroquine , ritonavir , famotidine etc.) are under clinical trial but conducting solid clinical trials is reportedly more difficult with increased public inquiry over readily available drugs[8] (Shaffer,

2020). A combination of drugs could be more effective; for example, a combination of antitussive noscapine and hydroxychloroquine showed a strong binding affinity to SARS-CoV-2 M^{pro} [9] (Kumar et al., 2020b). A tremendous number of studies are underway to determine the therapeutic use of antivirals (bemcentinib, chloroquine & hydroxychloroquine, lopinavir boosted with ritonavir and remdesivir) and immune modulators (anakinra and canakinumab, azithromycin, brensocatib, convalescent plasma, corticosteroids, interferon beta, ruxolitinib, mesenchymal stromal cells and sarilumab and tocilizumab) to treat COVID-19 [10](Connelly, 2020). Treatment of COVID-19 is medically unmet and designing potential drugs that could halt infection and disease progression is critical. Designing drugs that directly act on conserved enzymes like the main protease or 3C-like protease (M^{pro} or $3CL^{pro}$), papain-like protease (PL^{pro}), non-structural protein 12 (nsp12), and RNA-dependent RNA polymerase (RdRP) could be broad-spectrum and effective [11] (Zumla et al., 2016). Remdesivir is one of the antivirals under clinical trial for COVID-19 treatment with probable inhibition of RNA synthesis *via* targeting RdRP [12](Saha et al., 2020). In a randomized controlled trial of 1,062 patients, compared to a placebo, remdesivir significantly shortened the recovery time of adult COVID-19 patients, suggesting its therapeutic role [13] (Beigel et al., 2020). Its clinical effect on severely ill patients, however, is controversial.

Several studies combining structure-based, virtual, and high-throughput screening methods are currently underway to identify SARS-CoV-2 M^{pro} inhibitors [14] (Zhu et al., 2020). Many research studies on viruses such as HIV virus, Hepatitis C virus and Ebola virus have shown that the viral protease is the common target for the development of antiviral drugs [14–16] . Since, the main protease (Mpro) or 3CLPro) of coronavirus is conserved among the coronaviruses and it is mainly responsible for the vi- ral replication [17–18] . Thus, any inhibitors which inhibit the main protease (3CLpro or M pro) and block the replication of SARS-CoV-2 would be effective and specific measures for the development. of therapeutic agents or antiviral drugs against SARS-CoV-2 [19] . Again, it is well known that the development and discovery of new therapeutic agents or drugs by traditional methods is time consuming, costly and rigorous scientific *in-vivo* and *in-vitro* pro- cesses and therefore, to supplement the old traditional method, now a day, computer aided *in silico* techniques are gaining lot of importance for the designing and formulation of new therapeutic agents or drugs [20 -21] .

Curcumin is a bright yellow coloured pigment isolated by plants of the Curcuma longa species. It is the principal curcuminoid of turmeric, a member of the ginger family, Zingiberaceae. It is popular herbal supplement , cosmetics ingredient , food flavouring, and food coloring[1] agent. Since two hundred years turmeric powder used in the treatment of various inflammatory diseases. Chemically,curcumin is adiarylheptanoid,belonging to the group of curcuminiods, which are natural phenols, responsible for yellow colour of turmeric. It is a Keto –enol tautomer existing in enolic form in organic solvents like DMF, DMSO and in Keto form in water[2]. Turmeric contains curcumin , demethoxy curcumin and bis-demethoxy Curcumin (Curcuminoids). The curcumin/demethoxycurcumin / bis demethoxy curcumin ratio in turmeric is approximately 100:21:3.

Chemistry of Curcumin :

Curcumin incorporates a 7 carbon linker and three major functional groups like α, β – unsaturated , β-diketone moiety and an aromatic o - methoxy phenolic groups. [22] The aromatic ring system , which are phenols are connected by two α, β unsaturated carbonyl groups . The diketones form stable enols and are readily deprotonated to form enolates the α, β – unsaturated carbonyl groups . The diketones form stable enols and are readily deprotonated to form enolate ; the α, β – unsaturated carbonyl group is a Michael acceptor and undergoes nucleophilic addition reaction mechanism. Due to its hydrophobic nature of curcumin it is poorly soluble in water but it is completely soluble in organic solvent like DMF,DMSO, etc

Curcumin has been shown to be a powerful antioxidant, antiinflammatory [23-26] and anticarcinogenic agent [27-29].Curcumin also exhibit hypoglycemic(30-31), Cardioprotective [32, 33], and nephroprotective effects [34 ,35]

Curcumin, the yellow pigment in turmeric has high antioxidant activity. It is capable of scavenging a variety of reactive oxygen species including superoxide anion radical, hydrogen peroxide, hydroxyl radical ,singlet oxygen, nitric oxide and other organic free radicals. It is a potent inhibitor of reactive oxygen generating enzymes such as cycloooxygenase and lipooxygenase .Feeding curcumin in the diet inhibits forestomach , duodenal, and colon tumorigenesis . The antioxidant activity of Curcumin is greater than that of demethoxy curcumin and bis-demethoxy curcumin . Several invitro and invivo studies have shown a correction between the keto- enol structure of curcumin and their transition metal complexes. The presence of phenolic groups in the curcumin plays a very important role in antioxidant activity of curcumin[36-41]. Further the presence of a -OCH_3 in ortho position to the hydroxyl group as well as of a β – diketone species appears to aggravate the antioxidant activity of Curcumin (42,43)

Curcumin has emulative (mimetic) properties of SOD, the enzyme catalyzing the dismutation of super oxide anion into hydrogen peroxide and oxygen (44,45).Thus , the curcumin has the potential to protect lipids , Haemoglobin and DNA against oxidative degradation.

Indefinance of the various pharmacological activities ,the biological application of curcummin as a ameliorative (therapeutic) agent is limited due to its low bioavailability , poor water solubility, low serum levels , limited time distribution , fast metabolism and excretion (44) . Thus , a wide variety of synthetic derivatives of curcumin were synthesized in order to improve the bioavailability of drug, without drop off its antioxidant activity .These synthetic methods includes condensation of the central β-diketone unit with semicarbazide, thiosemicarbazide, hydrazine and hydroxyl amine (45-47) and coordinate with transition metal ions.

Literature reveals that curcumin forms complexes with many transition metal ions like Copper, Iron, Nickel, Zinc , Cobalt ,Manganese in 1:1 and 1:2 molar ratio , these complex These complexes have been shown to have better antioxidant activity than curcumin (48-50) and the products of substituted curcumin and their metal complexes have excellent antioxidant properties than Curcumin (51-54)

Recent research studies have demonstrated that curcumin and its transition metal complex show exceptional photocytotoxic activity and in almost all cases an increase in the anti tumoral activity of curcumin has been observed when curcumin binding to metal ions (55). The phototoxicity of curcumin has been assigned to the generation of reactive oxygen species(ROS) and singlet nascent oxygen during photo excitation phenomenon (56-59) However, the clinical applications of curcumin have been fatally hamper by its poor bioavailability and pharmacokinetic profile due to its hydrolytic instability under new various physiological conditions (60,61). The presence of β-diketone moiety in the curcumin structure furnishes its hydrolytically unstable nature . To improve the aqueous stability and consequently therapeutic efficacy of curcumin, diverse moderations of curcumin have been synthesized and tested. One very freshly and fortunate blueprint to address this, problem takes advantage of curcumin's transition metal ions binding property (62-77) .Binding of Curcumin to a metal ions via its β-diketone moiety drastically decreases the tendency of curcumin to undergo hydrolysis in an aqueous media, which could result in an improved bioavailability and therapeutic efficacy.

By appropriate selection of metal and the accompanying ligands in trilateral geometry , the metal complex can be administrated to hitting cancer cells without affecting normal cells, using this strategy. Several transition metal complex with metal ions such as Cu (II) , Co (III), Fe (III), Pt (II) Nd(III) with curcumin and a variety of coligands with electron withdrawing and electron donating groups have been synthesized and all these complexes have been shown to be budding photochemotherapeutic agents (78,79,80,81) .So, taking into consideration of various biological activities of transition metal complexes of curcumin and their derivatives, we report herein the synthesis and characterization of some coordination compounds of Cu^{2+} ion with a Curcumin acquired hydrazone Schiff base ligand derived from Carbohydrazide and curcumin which may show excellent antioxidant activity than curcumin..

2. Experimental Part

2.1 Material and physicochemical characterization

All required chemicals were purchased from Merck or Sigma Aldrich and used without further- purification. Carbon, hydrogen and nitrogen elements were determined using CHN elemental analyser from CIF lab of Jiwaji University Gwalior.

2.2 Volumetric Estimation of presence of copper metal in coordination complexes-

The Copper content was determined by volumetric analysis, based on the oxidation of iodide ions into I_2 by Cu^{2+} ions,which gets reduced to Cu^{+} [82] . In this experiment, the liberated I_2 was titrated with standard sodium thiosulphate solution. The samples were subjected to decompose with concentrated sulphuric acid and hydrogen peroxide and evaporate to dryness until the SO_3 gas were eliminated The left residue was resuspended with hot water and boiled to dissolve the salt completely and then transferred in to a conical flask and make up the volume in a volumetric flask.

Procedure: To a Cu^{2+} ion solution ,add 3-4 mL of 10% of potassium thiocynate solution and 0.2 to 0.5 gm of potassium iodide were added , then after vigorous shaking of solution , mixture was then titrated against standard N/100 sodium thiosulphate solution until the yellow brownish colour became clearly visible. Now add 5 ml Starch solution in the mixture with stirring and the titration was continued until the blue disappeared.

2.3 Spectroscopic characterization of ligand and coordinated Cu (II) complexes :

UV- Vis spectra of ligand and its coordinated copper (II) complexes were measured on a Perkin Elmer UV-Vis Lamda 25 spectrophotometer in the range of 200-900 nm . Infrared (IR) spectra (in potassium bromide palettes) were recorded on a Perkin Elmer FT-IR Spectrophotometer in the range of 4000-400 cm^{-1} .Thermal decomposition studies of copper complexes were performed on PCT-2A Thermobalance analyzer in static air atmosphere , at a heating rate of 10^0C/min from room temperature to 1000^0C. The conductivity measurement were carried out in DMSO 10^{-3}M) using Digisun electronic digital conductivity meter. 0.01 M KCl solution is used for calibration of conductivitymeter.

Total antioxidant capacity of coordinated copper (II) complexes using invitro antioxidant activity protocols. The antioxidant capacity of compounds was quantified by comparison with the standard substances like DPPH & ascorbic acid etc. and was given in equivalent units of standard.

2.4 Synthesis of Curcumin acquired hydrazone Schiff base ligand

For synthesis of hydrazone Schiff base ligand from curcumin and carbohydrazide in a 1:2 molar ration. Thus, a mixture of carbohydrazide (0.625 gm ,5 mmol) ,2 ml acetic acid and 15 ml ethanol was refluxed under continuous stirring until the complete desolution of reactants then add an ethanolic solution of curcumin powder (0.940g 2.5mmol in 15 ml ethanol). The resulting mixture was continuously stirred at 70-80^{0}C for 3 hours, when solid yellowish product was separated out . It was filtered off , washed several time with ethanol and air dried . Due to low yield of product , we facilitate to obtain the copper(II) complexes via template method , assuming that the Cu^{++} favours the condensation reaction , the ligand obtained was only used for the study of UV-Vis ,FT-IR , and antioxidant capacity testing .

The Curcumin acquired hydrazone Schiff base ligand was obtained by the condensation reaction of Curcumin with carbohydrazide in ethanol according to the literature [83]

Template synthesis of Copper (II) complexes –

Copper (II) complexes were prepared by the following procedure:

Carbohydrazide (2 m mol 0.4 gm) and 10 ml ethanol was refluxed until complete dissolution of reactant and resultant solution was stirred with an ethanolic solution of appropriate copper salt dissolved in minimum amount of ethanol - water :

$CuCl_2 .2H_2O$ (1 mmol, 0.171gm) Complex 1

$CuSO_4 .5H_2O$ (1 mmol, 0.185gm) Complex 2

$Cu(CH_3COO)_2 . H_2O$ (1 mmol, 0.212gm) for the Complex 3

The resulting solutions were continuous stirred under slight heating for 3-4 hours, when solid coloured product were precipitated then separated out. They were filtrated off , washed several times with ethanol and acetone and dried in a dessiccator .

Curcumin

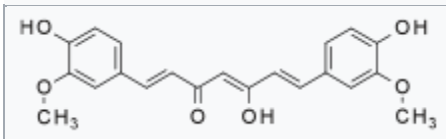

Enol form

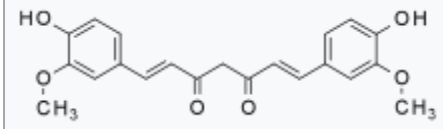

Keto form

IUPAC Name -(1*E*,6*E*)-1,7-Bis(4-hydroxy-3-methoxyphenyl)hepta-1,6-diene-3,5-dione
Figure -1 – Keto –Enol Form of Curcumin

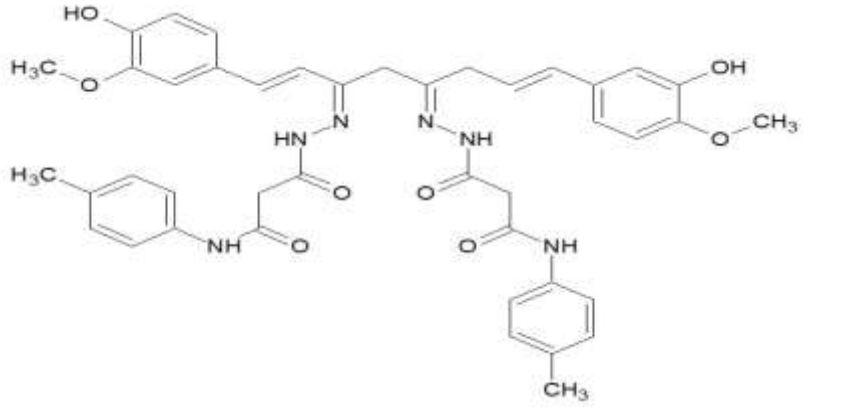

Figure -2 Structure of Curcumin Acquired Schiff base ligand

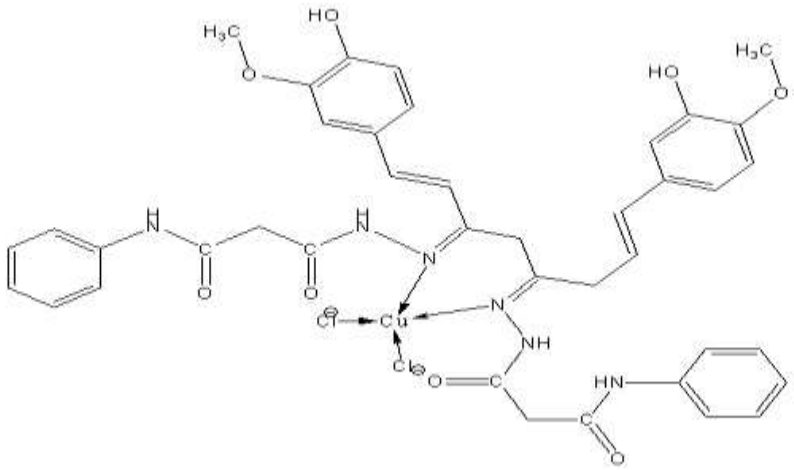

Figure-3 Structure of Coordinated [Cu $(H_2L)_2$ Cl_2]. $2H_2O$,

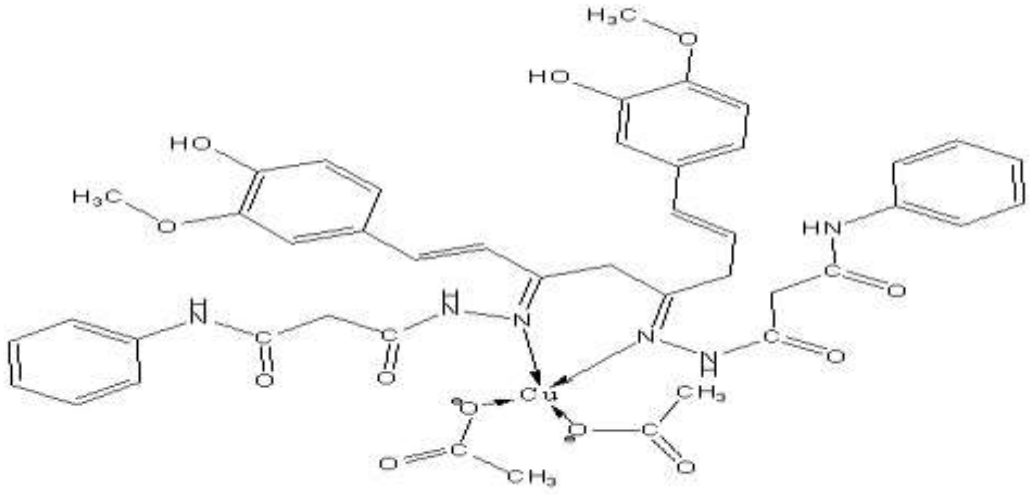

Figure -4 Structure of Coordinated [Cu $(H_2L)_2$ $(CH_3COO)_2$]$5H_2O$

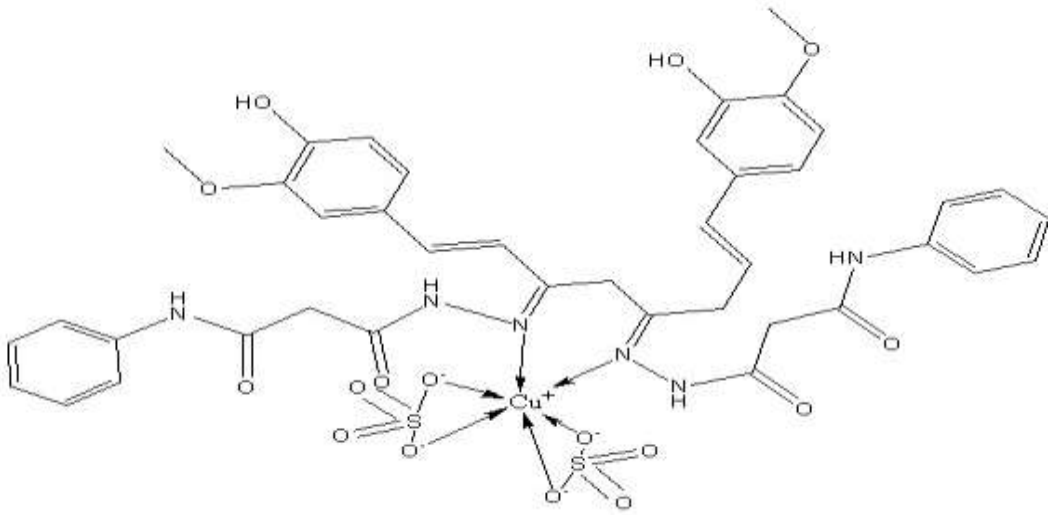

Figure -5 Structure of Coordinated Cu $(H_2L)_2$ $(SO_4)_2$].$5H_2O$

Antioxidant Activites -

2.5 Molecular Docking Studies

The X- ray crystallographic structure of main protease (M^{pro} PDB ID 6LU7) of SARS –CoV-2 has been downloaded from the protein data bank (PDB) (http:// www.pdb.org) data base. Preparation of protein for docking simulation was achieved by using Graphical user Interface Program "Auto Dock tools (ADT) 1.5.6" (Molecular Graphics Laboratory tool as MGL tool) developed by Scripps Researchers Institute [84]. Specific

chain length (chain A) of Protein (6LU7) has been selected for the preparation of receptor protein input file for docking study.

Receptor protein preparation for docking study was initiated by remaining water molecules, heteroatom and co-crystallized ligands from PDB crystal of Protein 6LU7, polar hydrogen atoms along with kollman united atom charges were added subaquently to the receptor protein input file and finally the receptor protein input file was saved as .Pdb file [85-87]. The three dimensional (3D) structure of ligand and Coordinated copper (II) complexes were drawn in Chemsketch (ACD/ structure Elucidator, version 12.01, Advanced Chemistry Development ,Inc. Toronto, Canada ,2014(http:// www. acdlabs.com), MM2 program incorporated in Chem Draw Ultra 8.0 were used for geometry optimization of all the compounds and finally, the geometry of all compounds were further optimized with the help of MOPAC6 package using the semi empirical AM1 Hamiltonian (88) and structure of all compounds were saved as .Pdb file .The input of .Pdbqt file of all the compounds the docking simulation was generated with the help of Auto Dock Tools (ADT) by assigning required Gasteiger charge and merging non-polar hydrogen.

The current research work is based on antioxidant activity of curcumin acquired Schiff base ligand and copper complex of the curcumin and to be evaluated against covid-19 with the help of molecular docking studies. Furthermore the molecular docking study is carried out on Schiff base ligands and complexes to identify the antioxidant capabilities through inhibition of main protease enzyme. As per our objectives, the three dimensional crystal structures of thymidylate synthase enzyme (PDB ID: 6LU7) was procured from protein data bank.

Molecular docking study was carried out using Autodock Vina as per the procedure adopted by Agrawal et al. (2020) and the docking parameters were defined as coordinates of the centre of binding site with x = -22.283, y = 12.599, z = 58.966 and in case of DNA gyrase, binding radius = 1.000 Å and the grid dimension used for all the three (3) proteins are 47.25 × 47.25 × 47.25 Å (grid size) with point separated by 1.000 Å (grid-point spacing).

2.6 Docking Study using auto dock Vina.

Auto dock Vina program 1.1.2 developed by Scripps Research institute were employed for all the molecular docking simulations and BIOVIA. Discovery studies 2020(DS) , version 20.1.0.0 (Dassault System BIOVIA, Discovery studio Modeling Environment, Release 2017, San diego: Dassault Systems 2016) and Edu Pymol version 1.7.4.4 were used for the visualization and analysis of docking results and corresponding intermolecular interactions between receptors and the compounds [53-54]. In order to eliminate any biasness arising during docking study blind docking of the compounds and into the protein were carried out by constructing three dimensional (3D) affinity (grid) maps and electrostatic grid boxes of dimension 50 X 50 X 50 A^0 grid point s and grid center (X,Y,Z) of -26.283 12.599 58.966 with a spacing of 1.00 A^0 with the help of Auto grid auxiliary program for each of the receptor to cover the entire active site and essential residues within the binding pocket [89]. Lamarckian generic algorithm was used for all docking simulation and all torsions were allowed to rotate.

3. RESULTS AND DISCUSSION

Curcumin acquired Schiff base ligand and its coordination complexes with Cu (II) ions are stable under ambient conditions. All compounds were soluble in common organic solvents like DMF, DMSO, hexane .All the compounds were characterized by elemental analysis , UV-Visible, FT-IR, Fluorescence spectroscopy .The first step of our research is the preparation of Curcumin acquired hydrazone schiff base ligand with hydrazine hydrate , with the formation of coloured 2-hydrazinocarbohydrazone according to literature (42).The condensation reaction of 2- hydrazino carbohydrazide with curcumin in a 2:1 molar ratio in ethanolic solution facilitate the formation of hydrazone Schiff base ligand whose empirical formula has been justified by FT-IR spectra and also confirmed by the analytical and spectral analysis of its copper complexes. Since literature reveals that Curcumin exists predominately in its enol form in polar solvents, the new synthesized

hydrazone ligand should have the structure l presented in fig. 2a. This compound results by the condensation reaction of carbonyl group and hydroxy ethanolic group of curcumin with primary amine group of two 2-hydrazinocarbohydrazide units. A tautomeric form is also possible in some metal complex fig.2b

FT-IR spectroscopy

The FTIR spectra of curcumin acquired hydrazone schiff base ligand the first change is observed it is disappearance of the sharp bands assigned to the stretching vibration ϒ(NH_2) 3562 cm^{-1} and ϒ (NH_2) 3307cm^{-1} of the primary amine group of 2-hydrazinocarbohydrazide and also appears new band due to C=O group conjugated with C=C of curcumin (1624-1608 cm^{-1}) .Along with these bands ,a new band located at 1682 cm^{-1} may be assigned to ν (C=N) of an imine functional group. The appearance of a medium absorption band around of 3589 Cm^{-1} is an indication >N secondary amine groups.

UV- Visible Spectroscopy:

The scanning of the spectra for the ligand was done from 200-700 nm. The maximum absorbance wavelength was observed from the data for the curcumin ,ligand and its coordination compounds with Cu^{2+} ions as shown in fig. 1 The absorption of these solutions was measured at 429 nm ,360 nm, 330 nm, 345 nm, and 325 nm. Ligand showed strong absorption band at higher frequency (360nm) which may be due to ∏-∏* transition. In the case of coordination complexes of copper (II) absorption band occur at 330, 345, and 325nm which may be due to n-∏ and ∏-∏ transition .In the case of coordination complex of copper (II) absorption band occurs at 330, 345, and 325 nm which may be due to **n-∏*** and ∏-∏* transition.

3.1 Chemical analysis of Coordination compound:

The interaction of hydrazone Schiff base ligand with copper (II) salts in ethanolic solution yields monomeric complex 1-3.

Analytical data:

a. **[Cu (H_2L)] $Cl_2.2H_2O$:** Light green solid, yield 85%, Melting point 260-280^{0}C, Molar conductance $Λ^{-1}mol^{-1}$ cm^2:22 Exp. % C: 49.91, H: 4.03, N: 10.14, Cu: 7.36,Calc. % C: 47.87, H: 3.97, N: 10.10, Cu: 7.38.
Selected IR data (ν cm-1) – 3237, 2245, 1631, 1671, 1189, 504, 494, UV-Vis (DMSO): λ max =330 nm

b.[Cu (H_2L)] $SO_4.5H_2O$: Brown solid, yield 72%, , Melting point 310-320 ^{0}C , Molar conductance $Λ^{-1}mol^{-1}$ cm^2: 20 , Exp. % C: 45.61, H: 4.03, N: 11.10, Cu: 7.65,Calc. % C: 55.2, H: 3.97, N: 11.02, Cu: 6.97,Selected IR data (ν cm-1) – 3435,3237, 2245, 1631, 1671, 1542, 1326, 1259,972,504,494 ,UV-Vis (DMSO): λ max = 345 nm

C.[Cu (H_2L)] ($CH_3COO)_2.5H_2O$: Dark Brown solid , yield 65%, , Melting point 315-317 ^{0}C , Molar conductance: $Λ^{-1}mol^{-1}$ cm^{-1}-18 , Exp. % C: 41.86, H: 4.46, N: 9.08, Cu: 6.95,Calc. % C: 41.26, H: 4.32, N: 8.96 , Cu : 6.02,
Selected IR data (ν cm^{-1}) – 3237, 2245, 1659, 1671,1631, 1524, 1339, 1259, 972, 810, 504, 494, UV-VIS (DMSO): λ max =325 nm.

Thus, the analytical data indicate that the coordinated cooper (II) compound form copper chloride , copper sulphate and copper acetate are in 1:1 metal ligand molar ratio . The composition of coordination compound is in accordance with the proposed empirical formula and these were further confirmed by the thermal decomposition studies.

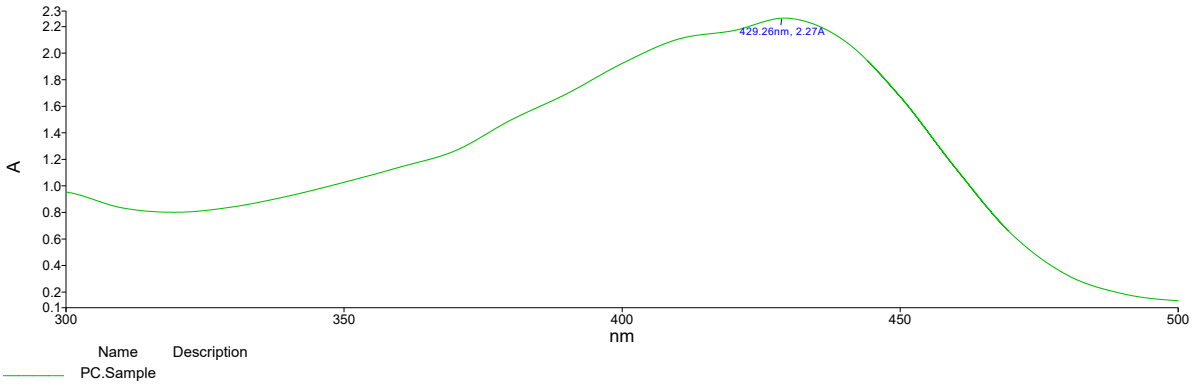

Figure -4 UV spectra of Pure curcumin powder

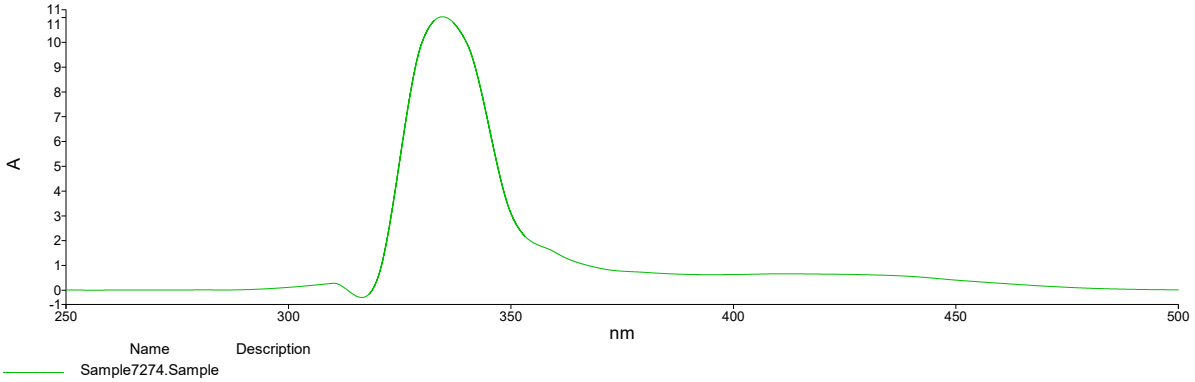

Figure -5 UV spectra of Schiff base Ligand

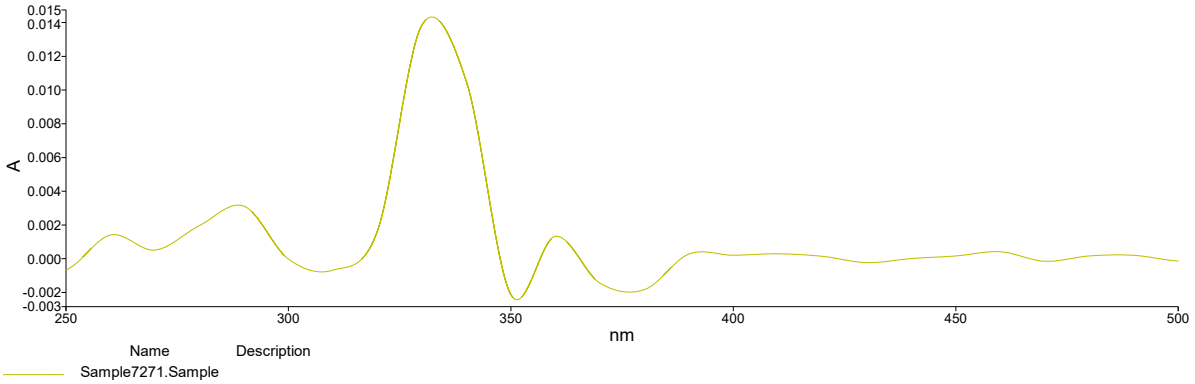

Figure -6 UV spectra of Copper complex 1

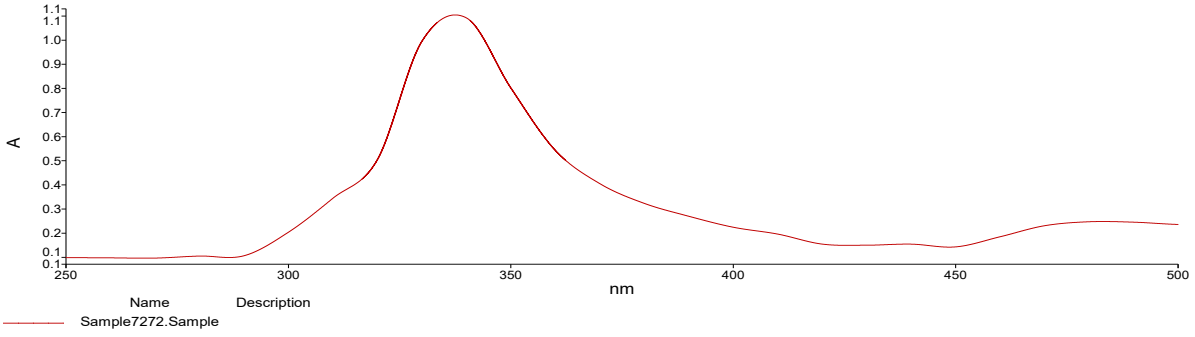

International Journal of Environmental Sciences
ISSN: 2229-7359
Vol. 11 No. 23s, 2025
https://theaspd.com/index.php

Figure- 7 – UV spectra of Complex -2

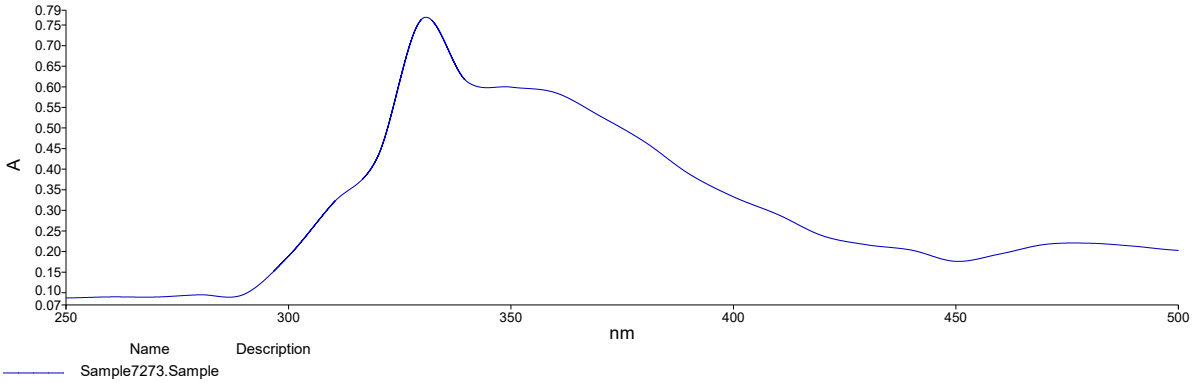

Figure -8 UV spectra of Complex -3

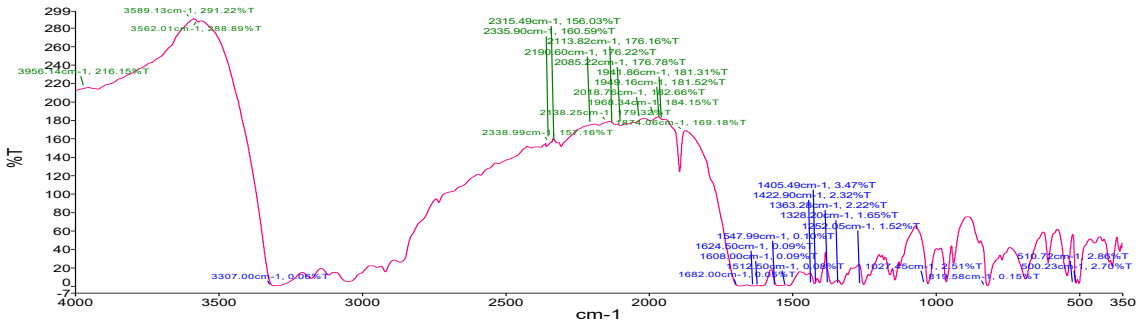

Figure – 9 FT-IR spectra of Schiff base ligand

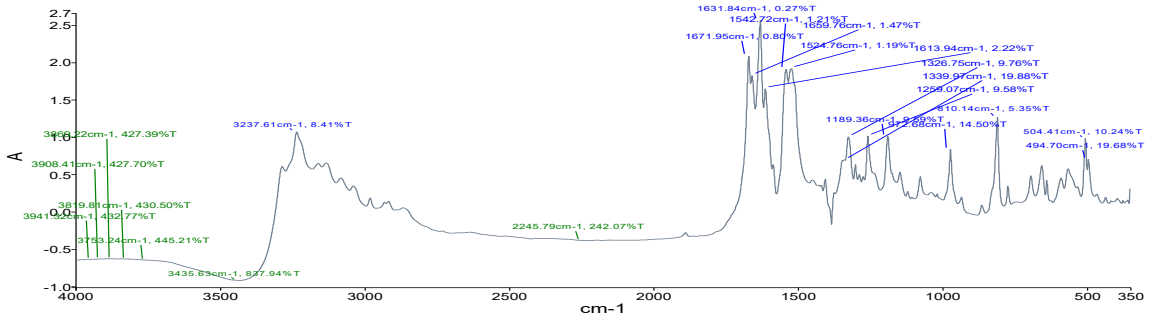

Figure -10 FT-IR spectra of Complex 1

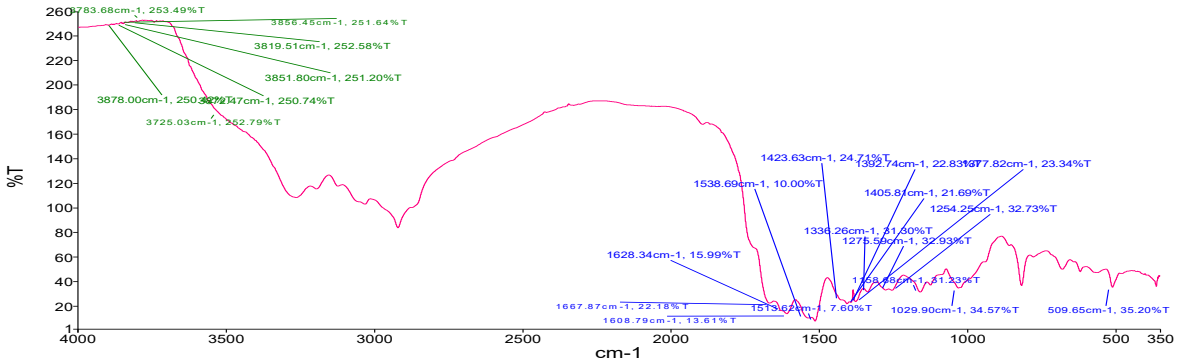

Figure -11 FT-IR spectra of Complex 2

International Journal of Environmental Sciences
ISSN: 2229-7359
Vol. 11 No. 23s, 2025
https://theaspd.com/index.php

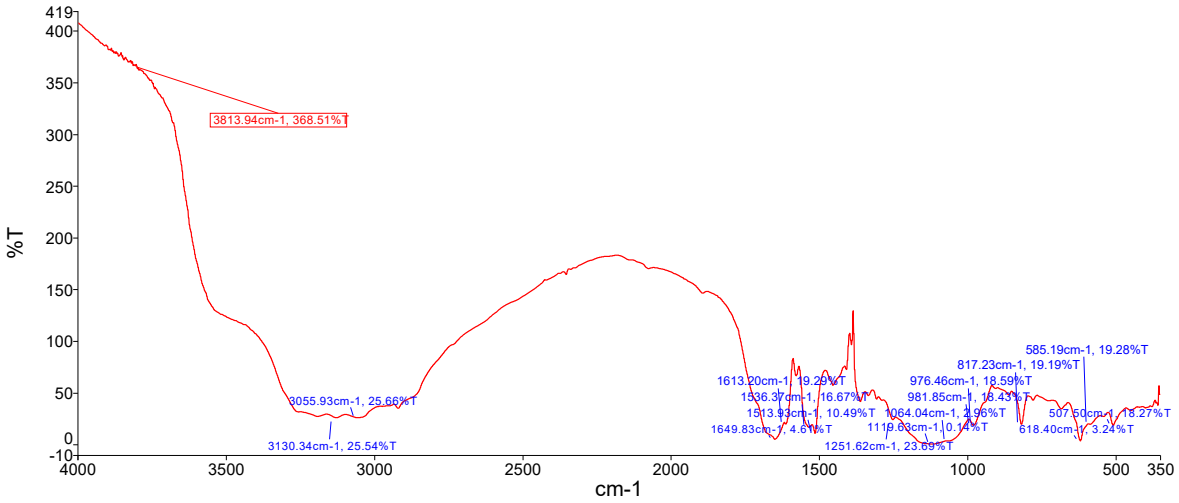

Figure -12 FT-IR spectra of Complex 3

3.2 Thermal behaviour of Coordination compounds:

The results of the thermal analysis for the coordination compounds in the table 1 and the thermogram are shown in the supplementary data Fig.13 ,14 The coordinated copper(II) complexes are stable at room temperature and did not change the colour in safekeeping in a dry place.

The thermal decomposition of the complexes take place in four steps. The first decomposition step , an endothermic one, in the temperature range of 80^0C-130^0C is associated for all complexes to the loss of crystalline water (90-92). The second step of the thermal decomposition of the complexes corresponds to the elimination of coordinated water and takes place over a temperature range of 140^0C-220 ^{0}C ,associated by an endothermic peak .For the complexes, second step can be correlated with the ligand side group releases , phenolic groups of ligand for complex ,weight loss in accordance with the elimination of two water molecule. In the next step of decomposition is a complex reaction step , being an overlap of process. The third stage of thermal decomposition process corresponding to the loss of chloride , sulphate and acetate ions [93]. The last step of thermal decomposition was strongly exothermic corresponding to the oxidative degradation of the organic ligand residue. It starts from 380 to 490^0 C and finishes around 750^0 C for all the complexes. The final residue of decomposition is Cu O and the copper percentage determine from this is in accordance with the theoretical content.

Table 1 -Thermal Decomposition data for the Copper (II) Complexes

Complex	Step	Thermal effect	Temperature range (^{0}C)	%Δm $_{exp.}$	%Δm $_{calc.}$	Chemical Process
1	I	Endothermic	80-130^{0}C	1.82	2.10	H_2O Loss
	II	Endothermic	110-210^{0}C	3.4	4.32	$2H_2O$ Coordinated Loss
	III	Exothermic	210-360^{0}C	19.1	19.25	2HCl +$2H_2O$ Loss
	IV	Exothermic	360-780^{0}C	65.00	65.66	Oxidative degradation of organic residue
II	I	Endothermic	60-80^{0}C	1.94	2.20	H_2O Loss
	II	Endothermic	160-220^{0}C	3.9	4.85	$2H_2O$ Coordinate Loss

	III	Exothermic	230-490^{0}C	22.4	24.2	Loss of SO_4^{-2} ions
	IV	Exothermic	490-750^{0}C	54.00	56.00	Oxidative degradation of organic residue
III	I	Endothermic	70-90^{0}C	2.12	2.90	Loss of H_2O molecules
	II	Endothermic	120-190^{0}C	5.20	5.68	$5H_2O$ Loss
	III	Exothermic	200-400^{0}C	24.4	25.2	Loss of acetate ions
	IV	Exothermic	400-790^{0}C	49.2	52.4	Oxidative degradation of organic residue

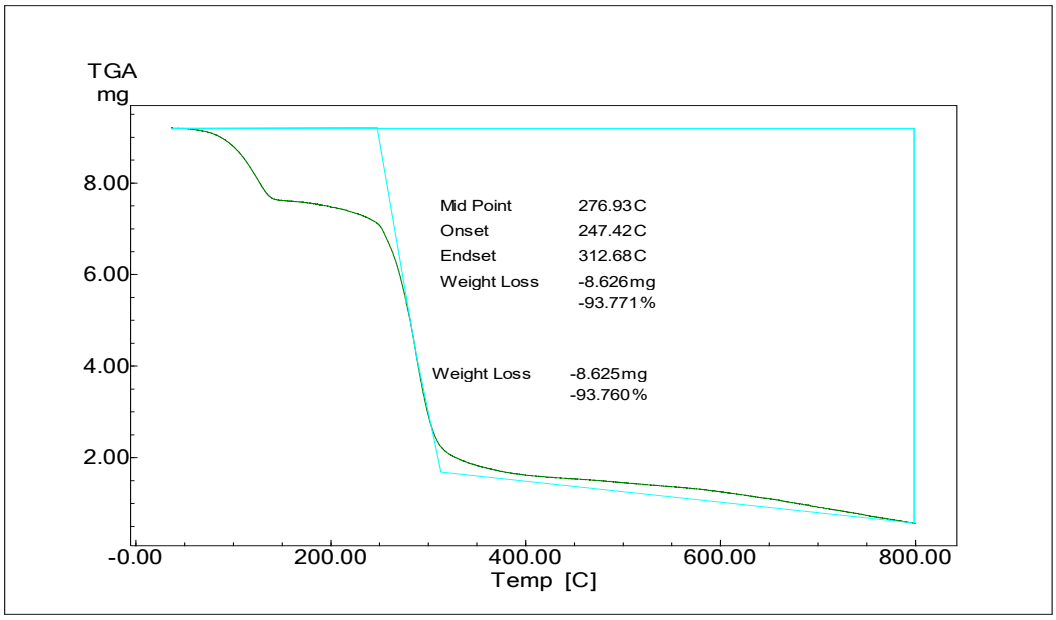

Figure 13 - TGA spectra of Schiff base ligand

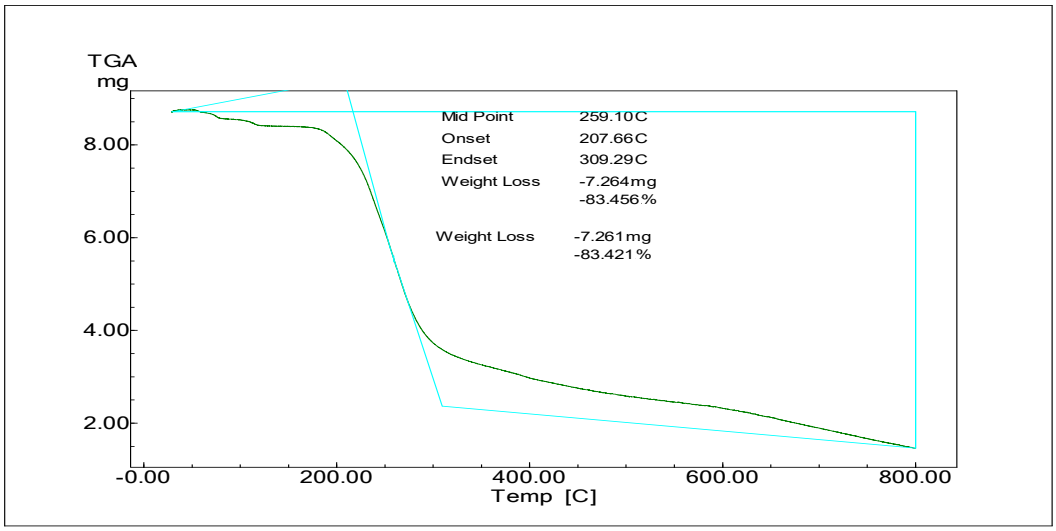

Figure 14 - TGA spectra of Coordinated Copper (II) Complex

3.3 Infrared Spectra

The comparative study of IR spectra of coordinated copper (II) complexes with those of the ligand of Curcumin proves ligand formation and allow to establish the groups involved in the coordination to the Cu^{2+} ions . The most important infrared bands for ligand and coordinated Cu(II) complex are reported in table 2 and the IR spectra of the ligand and Cu (II) complexes are present in the supplementary material (Fig.9,10,11,12)

The IR spectrum of ligand shows in the region of higher wave numbers two characteristics bands 3562 and 3307 cm^{-1}) assigned to the stretching vibration ν_{asym}(NH_2) and ν_{sym}(NH_2) of the primary amine group [94,95]. The absence of these bands in the IR spectra of copper complexes is consistent with the condensation of primary aromatic amine groups from two units of ligand with >C=O and –OH enolic groups of curcumin in the presence of Cu^{2+} ion. This result is also supported by the disappearance of the band due to the inplane deformation vibration of amino group ,δ (NH_2) 1613 cm^{-1} : in the spectra of all copper (II) complexes.

In the region of higher wave numbers, the IR spectrum of curcumin acquired Schiff base ligand shows a strong sharp peak at 3562 cm^{-1} and a broad IR band with maximum around
3307 cm^{-1} ; these are assigned to the stretching vibrations of the O-H band in phenolic groups and the enolic -OH group respectively.[96,97].The position and the characteristic features of last band i.e. enolic OH group related to the stretching of intramolecular hydrogen bond of the enol group.

In the infrared spectra of all copper (II) complexes this infrared region is dominated by a strong and broad band around 3435- 3055 cm^{-1} assigned to ν (OH) of coordinated /crystalline water molecule [98,99] Curcumin acquired hydrazone Schiff base lignd has two strong stretching bands at 1624 cm^{-1} and 1608 cm^{-1} , which corresponds to the mixture of stretching vibrations of C=O group conjugated with C=C double bond[100] ,The disappearance of these bands and the appearance of a medium intensity band located at 1628 - 1631 cm^{-1} in the spectra of the copper complexes which may be assigned to ν(C=N) stretching vibrations confirm the condensation of carbonyl group and formation of a hydrazone schiff base ligand [101-103] .

The band due to the stretching vibration of C-O lying at 1157cm^{-1} in the enolic spectrum of ligand, is absent in the spectra of all copper (II) complexes. This observation and also the appearance of a new band at 1631-1671 cm^{-1} for the copper complexes which may be due to ν($C_{aliphatic}$ N) confirm the condensation of the OH enolic group of ligand with the $–NH_2$ group of Carbohydrazide.

Table 2 -Characteristic bands in the IR spectra of Curcumin acquired hydrazone schiff base ligand and Copper(II) complexes (ν_{max} ,cm^{-1})

Hydrazone Schiff base ligand	Complex -1	Complex-2	Complex -3	Assignments
-	3435 m	3348 m	3130 m	ν_{asym}(NH_2)
3307 s	3237	-	-	ν_{sym}(NH_2)
3562 s	-	-	-	ν (OH) enol
-	-	-	-	ν (OH) phenol
1624 s	1659 m	-	-	ν (OH) H_2O
1606 s	-	-	-	δ NH_2
1547 s	-	1649 m	1667 m	ν (C=O) & ν (C=C)
1405 s	1542 vs	1631 m	1628 m	ν C=N (endo)
1272 s	1401 s	1613 m	1608 m	ν_{asym}(C- CH_3)
1149 s	1259 m	1540 vs	1513 vs	ν (C-O) Phenolic
-	1189 m	1450 s	1423 m	ν (C-O) enolic

-	-	1280 m	1254 m	ν($C_{aliphatic}$ N)
-	-	1162 m	1119 m	ν (-Cl)
-	-	1064 m	1029	ν ($-SO_4^{--}$)
1027 s	1032 m			ν ($-CH_3COO^-$)

s=strong , v s =very strong ,m=medium ,ms= medium strong

All copper complexes show strong absorption band around 1272-1280 cm^{-1}assigened to ν_{asym}(C-O) phenolic curcumin schiff base ligand and these remain unaffected in the spectra of all copper complexes (104,105,106).

From the result of IR Spectra although the position of $\nu(NH_2)$ band is difficult to identify due to overlap with ν(-OH) band ,the involvement of the NH group (NH bonded to aliphatic carbon of Curcumin) in coordination can be presumed on the base of the stereochemistry of the complexes. From the spectral analysis of the IR spectra we can conclude that the ligand act as hexadentate NNOOOO in all copper complexes. Due to complexity of the IR spectra, it is not possible to establish the neutral dibasic or tetrabasic nature of the ligand in the complexes but this one was presumed.

3.4 Electronic Spectral data

Electronic spectral of Curcumin, hydrazone Schiff base ligand and Copper (II) coordination complexes were recorded in solid state as well as in DMSO: water solution, The Spectra were recorded on the solution to be used to determine antioxidant capacity but diluted to a 1:40 DMSO water ratio. The UV-Vis spectrum of Curcumin in solid state displays a strong absorption band at 429 nm, due to n-[]* transition. The electronic spectrum of hydrazone schiff base ligand show strong band at 340nm .Compared to curcumin the hydrazone ligand exhibits maximum absorption band at 345 nm indicating that the curcumin chromophore is involved in the reaction with carbohydrazide .Diffuse reflectance UV-Vis Spectra of the Copper (II) complexes show a broad and relatively intense band in the range of 325 at 370 nm with a maximum at 345 nm (complex 1), 370 nm (complex 2) and 360 nm (complex 3) .In addition , the spectra of all copper (II) complexes show new bands in the visible region ($4000A^0$-$8000A^0$)due to d-d transition of Copper ions. The visible absorption bands for the copper complexes are in accordance with a distorted octahedral , geometry around the Cu^{2+}ion with a broad band at 16686 cm^{-1}(Complex 1) assigned to $^2B_{1g} \rightarrow {}^2E_g$,14,275 cm^{-1} and 18,280 cm^{-1} due to $^2B_{1g} \rightarrow {}^2B_{2g}$ and $^2B_{1g} \rightarrow {}^2E_g$ ((for complex 2 and 3 respectively [107]

In complex 1 and 2 the cooper ions are tetra coordinated and taking into account of donor oxygen and nitrogen atoms and the maxima of the visible bands, the most probable symmetry is square-plane (D_4 h) for the remaining complex (3). Thus, the electronic spectrum of complex 2 exhibits three absorption bands which may be assigned to d-d transition in D4h symmetry :12,600 cm^{-1} assigned to $^2B_{1g} \rightarrow {}^2B_{2g}$,16180 cm^{-1} assigned to $^2B_{1g} \rightarrow {}^2E_g$ and 24,000 cm^{-1} assigned to $^2B_{1g} \rightarrow {}^2A_{1g}$. On change transfer phenomenon [108] .In the case of complex (3) the electronic spectrum show a single visible band whose maximum at 14980 cm^{-1} can be attributed to the transition $^2B_2 \rightarrow {}^2B_1$ in D_{2d} symmetry [107]

Pure Curcumin in DMSO: water solution showed the same UV-Vis broad band , with a maximum at 429 nm while the maximum absorption band for the ligand appeared at 340 nm . This last band was almost unaffected in spectra of all Cu(II) complexes . The high intensity of the ligand bands at 340 nm , 220 nm, and 210 nm make the bands characteristics of d-d transition not detectable. Taking into account that the hydrazone schiff base ligand characteristic bands were showed in the spectra of the all copper complexes and their colour remains in solution, it can be assumed that all the coordinated copper complexes maintain their structure in DMSO: water solution.

3.5 Antioxidant activity:

Total antioxidant activity of curcumin, hydrazone ligand and coordinated copper (II) complexes was evaluated by DPPH method and total phenolic compounds by UV-Visible spectrophotometer and quantified by comparison with standard DPPH as equivalent units of standard substances according to the recommended protocols . A stock solution was prepared by dissolving 0.25 g powdered compound in 100 ml ethanol p.a..

From the stock solution; a working volume of 5 µl was taken according to standard procedure. The solutions were diluted with methyl alcohol of high purity – the specific reagent of the method. For curcumin, ligand and coordinated copper (II) complexes, we made determination on the stock solution and on the samples with the best values of total antioxidant activity.

As we can see from the result of the total antioxidant capacity of each compound, presented in table 3 .The antioxidant capacity of coordinated copper(II) complexes is higher than that of curcumin and of the hydrazone Schiff base ligand and it is strongly influenced by the Copper ions: ligand molar ratio , Complex 1 showed the highest antioxidant activity in DPPH assay . Complex 2 do not show significant antioxidant activity but it also have better antioxidant activity than Curcumin and hydrazone Schiff base ligand.

Table 3 Representative antioxidant activity of Curcumin , hydrazone schiff base ligand and their Copper (II) complexes

Compound	Dilution factor of stock solution	Inhibition	DPPH Equivalent antioxidant Capacity	Total antioxidant activity(%)
Curcumin	1ml	0.632	3.555	17.07
Ligand	1ml	0.787	2.064	11.61
Complex 1	1ml	0.926	1.468	11.97
Complex 2	1 ml	0.460	1.957	13.977
Complex 3	1 ml	0.797	1.765	12.76

3.6 Molecular Docking Analysis –

Current molecular docking studies revealed that complexes and Schiff base ligands both properly interacted with target i.e main protease (M^{pro}) of SARS-CoV-2. Recent findings suggested that this particular enzyme is made up of three domains having different amino acids residues vis. main viz., domain I (residues 8–101), domain II (residues 102–184) and domain III (residues 201–303) and as similar to other coronaviruses, SARS-CoV-2 Mpro also consist a Cys145-His41 catalytic dyad located in a cleft between domain I and domain II (Chhetri et al. 2021). Moreover, in recent published literatures suggested that three specific residues viz. His41, Cys145, and Glu166 are important for interactions and inhibition of this target enzyme. In this study, both synthetic ligands (copper complex and curcumin acquired Schiff base ligand) could interact with enzyme in domain I and domain II and could demonstrate significant binding affinity towards target, i.e. -9.5 and -8.7 kcal/mol respectively. Although both molecules could not interact with above mentioned three amino acids which are supposed to be mandatory for inhibition of enzyme but other interactions afforded by both ligands could not be ignored as till date no specific inhibitors or other approaches found be effective in treatment of covid-19 and both molecules have shown potent antioxidant activity in intro conditions. We are emphasizing here on antioxidant activity with the treatment of covid-19 because antioxidants are proven therapy in overcoming the symptoms of covid-19. This molecular docking study also conclude here that not only the active site but other sites in the target enzyme might be a reasonable areas where interactions can be investigated for development of better therapeutic agents for treatment of covid-19 [108].

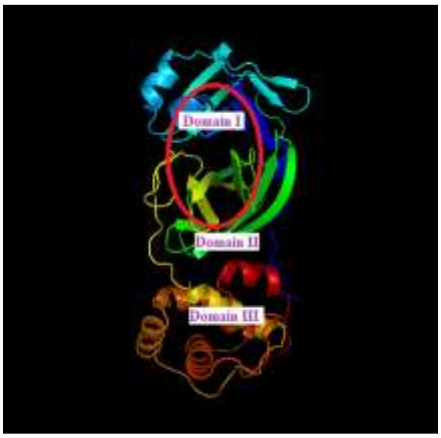

Fig. 15 . Structure (Chain A) of M pro of SARS-Cov-2 with domain I, II and III (Red circle represents the catalytically active site of M pro).

Table 3 - Result of docking studies of Schiff Base Ligands and its copper (II) complex

Name	Binding Affinities (kcal/mol) with targets	Amino acids Involved in the interactions	H-bond with Distance
		PDB=6LU7	
complex1 curcumin acquired Schiff base	-9.5	Lys137, Asp197, Thr199, Tyr237, Tyr239, Leu287, Asp289, Glu290	1_out: :UNL1:N,6lu7:A:TYR 239:OH,1_out: :UNL1:H 2.079Å
	8.7	Val104, Leu106, Pro108, Gln110, Asn151, Val202, His246, Ile249, Pro293, Phe294	NIL

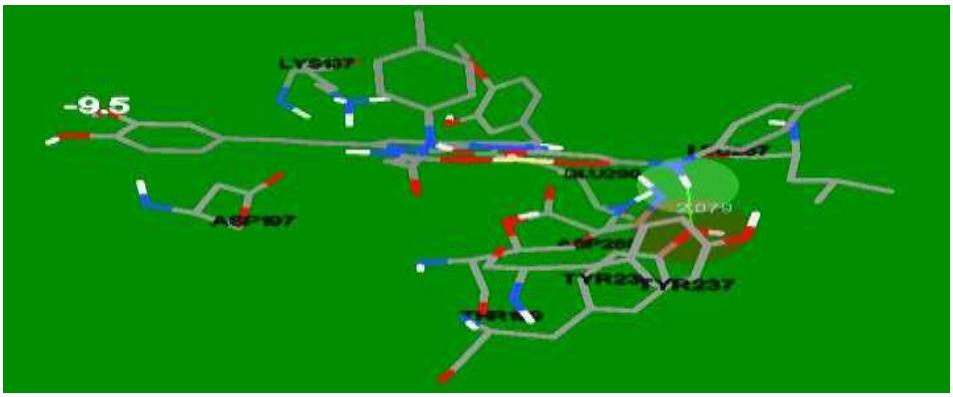

Fig. 16 - Molecular Docking Studies of Schiff Base ligand

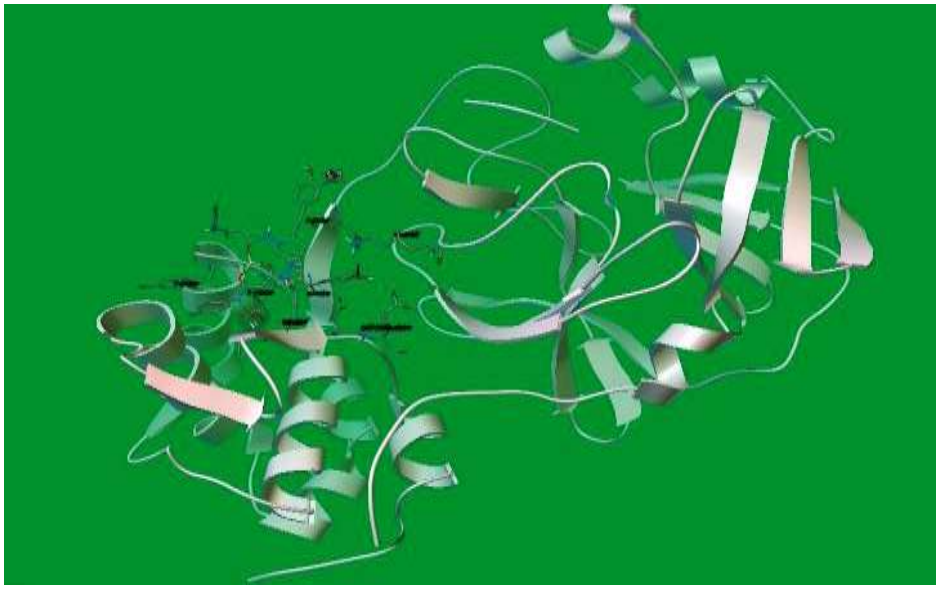

Fig.17 - Three dimensional images of interactions of complex with covid protease enzyme

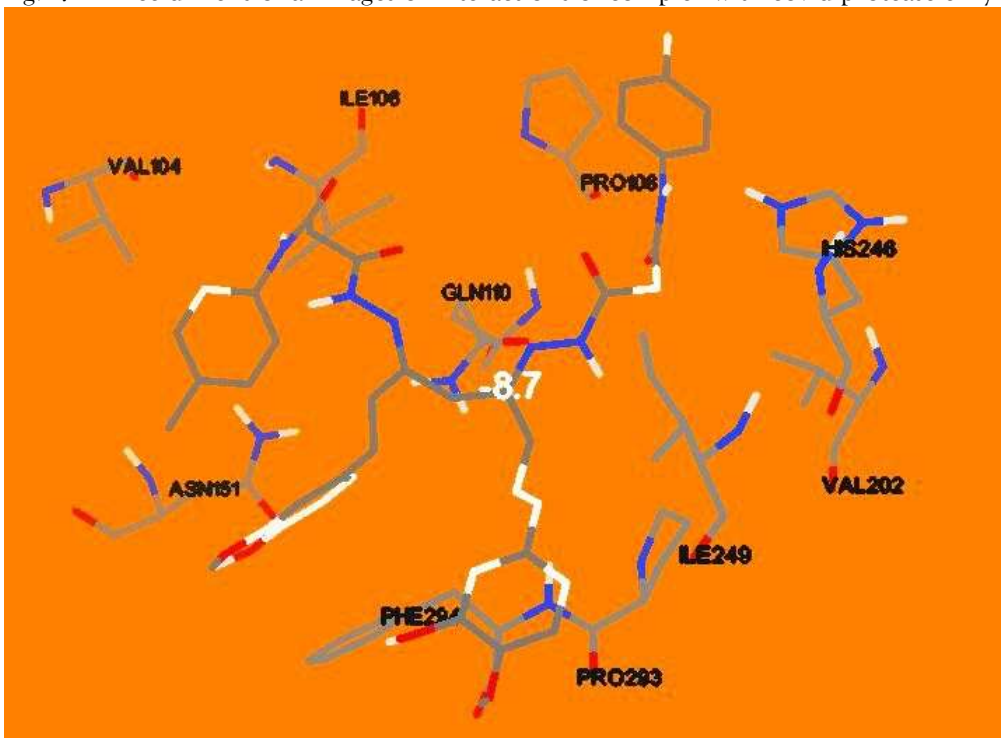

Figure- 18 Visualization of docking of Ligand L1 docked in M pro (6LU7): (A) Best binding mode of protein (Ligand L1 as green and blue stick), (B) Amino acid residues involved in hydrogen bonding interaction (dash line represents H-bonding, purple and blue colour represents donor and acceptor) and (C) Binding interaction (2D) of ligand L1 with amino acid residues of protein 6LU7 (dash line represents H-bonding and black dash line represents unfavorable acceptor-aceptor interaction).

Fig.19 - Three dimensional images of interactions of curcumin acquired Schiff base with covid protease enzyme .

4. Conclusion

Novel three copper (II) coordinated compounds have been prepared by template synthesis using curcumin , hydrazone schiff base ligand and appropriate copper salts in 2:2:1 molar ratio . Physiochemical, analytical, thermal analysis and various spectroscopic characterization confirmed the coordination of hydrazone schiff base ligand with Cu (II) ions in 2:2:1 molar ratio . All coordinated copper (II) complexes are better scavengers of superoxide anions radical than curcumin . This scavenging activity is mainly due to the redox reaction within the Cu^{2+}/ Cu couple and secondly to the phenolic functional group of the curcumin derivative hydrazone schiff base ligand. This research work also explain the fact that the copper complex exhibit the highest antioxidant activity. Molecular docking study of all the synthesized derivatives have been studied against the main protease (6LU7) of SARS - COV-2. The docking result explained various type of protein – ligand interaction and it is also seen that the ligands show significant interaction at the interface between domain I and domain II . Furthermost, most of the compounds showed interaction at the Cys 145 – His 41 catalytic dyad. The pharmacokinetic study (ADMET) has revealed that the ligand and coordinated copper (II) complexes could act as a potential drug candidate. Therefore we may conclude that the ligand and its coordinated copper complexes could act as potential inhibitor against the main protease of SARS – CoV -2 follows the order complex 1 > complex 3>complex 2. This research work did not receive any specific grant from funding agencies in the public , commercial or not-for - profit sectors.

Declaration of Competing Interest

The authors do not declare any conflict of interest. The authors declare no conflict of interest associated with this article and also no significant financial support has been received by us for preparing this manuscript**.**

Credit authorship contribution statement

Richa Kothari: Conceptualization, Designing, Formal analysis, Funding acquisition, methodology, writing original draft, writing review & editing.

Anurag Agrwal: Methodology, writing original draft, software supervision, Validation, visualization, writing review, editing.

Acknowledgment:
The authors are grateful to the research facilities available at the sophisticated instrumentation research laboratory, ITM university Gwalior. All the authors sincerely acknowledge CIF, Jjiwaji University Gwalior for elemental analysis.

REFERENCES

1.Huang, C., Wang, Y., Li, X., Ren, L., Zhao, J., Hu, Y., et al. (2020). Clinical features of patients infected with 2019 novel coronavirus in Wuhan, China. *The lancet* 395 (10223), 497–506. doi:10.1016/S0140-6736(20)30183-5

2. Patel, K. P., Vunnam, S. R., Patel, P. A., Krill, K. L., Korbitz, P. M., Gallagher, J. P., et al. (2020). Transmission of SARS-CoV-2: an update of current literature. *Eur. J. Clin. Microbiol. Infect. Dis.* 39 (1), 1–7. doi:10.1007/s10096-020-03961-1

3. Chow, N., Fleming-Dutra, K., Gierke, R., and Hall, A. (2020). Preliminary estimates of the prevalence of selected underlying health conditions among patients with coronavirus disease 2019—United States, February 12–March 28, 2020. *Morbidity Mortality Weekly Rep.* 69 (13), 382. doi:10.15585/mmwr.mm6913e2

4. Zhang, W., Du, R.-H., Li, B., Zheng, X.-S., Yang, X.-L., Hu, B., et al. (2020c). Molecular and serological investigation of 2019-nCoV infected patients: implication of multiple shedding routes. *Emerging microbes & infections* 9 (1), 386–389. doi:10.1080/22221751.2020.1729071

5. Cascella, M., Rajnik, M., Cuomo, A., Dulebohn, S. C., and Di Napoli, R. (2020). *Features, evaluation and treatment coronavirus (COVID-19) Statpearls*. Florida: StatPearls Publishing.

6. Chen, N., Zhou, M., Dong, X., Qu, J., Gong, F., Han, Y., et al. (2020a). Epidemiological and clinical characteristics of 99 cases of 2019 novel coronavirus pneumonia in Wuhan, China: a descriptive study. *The lancet* 395 (10223), 507–513. doi:10.1016/S0140-6736(20)30211-7

7. Gattinoni, L., Coppola, S., Cressoni, M., Busana, M., Rossi, S., and Chiumello, D. (2020). COVID-19 does not lead to a "typical" acute respiratory distress syndrome. *Am. J. Respir. Crit. Care Med.* 201 (10), 1299–1300. doi:10.1164/rccm.202003-0817LE

8. Shaffer, L. (2020). 15 drugs being tested to treat COVID-19 and how they would work. *Nat. Med. News Feature.* 1-1 doi:10.1038/d41591-020-00019-9. Kumar, N., Awasthi, A., Kumari, A., Sood, D., Jain, P., Singh, T., et al. (2020b). Antitussive noscapine and antiviral drug conjugates as arsenal against COVID-19: a comprehensive chemoinformatics analysis. *J. Biomol. Struct. Dyn.* 1–16. doi:10.1080/07391102.2020.1808072

10. Connelly, D. (2020). Targeting COVID-19: the drugs being fast-tracked through clinical trials and how they work. *Pharm. J.* 304 (7937), 312–313. doi:10.1211/PJ.2020.2020794

11. Zumla, A., Chan, J. F., Azhar, E. I., Hui, D. S., and Yuen, K. Y. (2016). Coronaviruses - drug discovery and therapeutic options. *Nat. Rev. Drug Discov.* 15 (5), 327–347. doi:10.1038/nrd.2015.37

12. Saha, A., Sharma, A. R., Bhattacharya, M., Sharma, G., Lee, S.-S., and Chakraborty, C. (2020). Probable molecular mechanism of remdesivir for the treatment of COVID-19: need to Know more. *Archives Med. Res.* 51 (6), 585–586. doi:10.1016/j.arcmed.2020.05.001

13. Beigel, J. H., Tomashek, K. M., Dodd, L. E., Mehta, A. K., Zingman, B. S., Kalil, A. C., et al. (2020). Remdesivir for the treatment of Covid-19. *New Engl. J. Med.* 383 (19), 1813–1826. doi:10.1056/NEJMoa2007764

14. Zhu, G., Zhu, C., Zhu, Y., and Sun, F. (2020). Minireview of progress in the structural study of SARS-CoV-2 proteins. *Curr. Res. Microb. Sci.* 1, 53–61. doi:10.1016/j.crmicr.2020.06.003

15. Lv Z., Chu Y., Wang Y. HIV protease inhibitors: a review of molecular selectivity and toxicity. *HIV/AIDS (Auckland, New Zealand)* 2015;7:95–104. doi: 10.2147/HIV.S79956. [PMC free article] [PubMed] [CrossRef] [Google Scholar]

16. de Leuw P., Stephan C. Protease inhibitors for the treatment of hepatitis C virus infection. *GMS Infect. Dis.* 2017;5:1–14. doi: 10.3205/id000034. Doc08. [PMC free article] [PubMed] [CrossRef] [Google Scholar]

17. Nishimura H., Yamaya M. A Synthetic Serine Protease Inhibitor, Nafamostat Mesilate, Is a Drug Potentially Applicable to the Treatment of Ebola Virus Disease. *The Tohoku J. Exp. Med.* 2015;237(1):45–50. doi: 10.1620/tjem.237.45. [PubMed] [CrossRef] [Google Scholar]

18Zumla A., Chan J.F., Azhar E.I., Hui D.S., Yuen K.Y. Coronaviruses - drug discovery and therapeutic options. *Nat. Rev. Drug. Discov.* 2016;15(5):327–347. doi: 10.1038/nrd.2015.37. [PMC free article] [PubMed] [CrossRef] [Google Scholar]

19. Shirato K., Kawase M., Matsuyama S. Middle East respiratory syndrome coronavirus infection mediated by the transmembrane serine protease tmprss2. *J. Virol.* 2013;87(23):12552–12561. doi: 10.1128/JVI.01890-13. [PMC free article] [PubMed] [CrossRef] [Google Scholar]

20. Hatada R., Okuwaki K., Mochizuki Y., Handa Y., Fukuzawa K., Komeiji Y., Okiyama Y., Tanaka S. Fragment molecular orbital based interaction analyses on COVID-19 main protease- inhibitor N3 complex (PDB ID: 6LU7) *J. Chem. Inf. Model.* 2020;60(7):3593–3602. doi: 10.1021/acs.jcim.0c00283. [PMC free article] [PubMed] [CrossRef] [Google Scholar]

21. ul Qamar M.T., Maryam A., Muneer I., Xing F., Ashfaq U.A., Khan F.A., Anwar F., Geesi M.H., Khalid R.R., Rauf S.A., Siddique A.R. Computational screening of medicinal plant phytochemicals to discover potent pan-serotype inhibitors against dengue virus. *Sci. Rep.* 2019;9(1):1–16. doi: 10.1038/s41598-018-38450-1. [PMC free article] [PubMed] [CrossRef] [Google Scholar]
22. ul Qamar M.T., Saleem S., Ashfaq U.A., Bari A., Anwar F, Alqahtani S. Epitope-based peptide vaccine design and target site depiction against Middle East Respiratory Syndrome Coronavirus: an immune-informatics study. *J. Transl. Med.* 2019;17(362):1–14. doi: 10.1186/s12967-019-2116-8. [PMC free article] [PubMed] [CrossRef] [Google Scholar]
23. [1] M. Heger, R.F. van Golen, M. Broekgaarden, M.C. Michel, The molecular basis for the pharmacokinetics and pharmacodynamics of curcumin and its metabolites in relation to cancer, Pharmacol. Rev. 66 (2014) 222–307.
[24] A. Kumar, M. Singh, P.P. Singh, S.K. Singh, P. Raj, K.D. Pandey, Antioxidant efficacy and curcumin content of turmeric (CURCUMA-LONGA L.) flower, Int. J. Curr. Pharm. Res. 8(2016) 112–114.
[25] M. Asouri, R. Ataee, A.A. Ahmadi, A. Amini, M.R. Moshaei, Antioxidant and free radical scavenging activities of curcumin, Asian J. Chem. 25 (2013) 7593–7595.
[26] M. Subramanian, M.N.A. Sreejayan Rao, T.P.A. Devasagyam,.B.B. Singh, Diminution of singlet oxygen-induced DNA damage by curcumin and related antioxidants, Mutat. Res. 311 (1994),249–255.
[27] K.I. Priyadarsini, Free radical reactions of curcumin in membrane models, Free Radic. Biol. Med. 23 (1997) 838–843.
[28] (a) A. Allegra, V. Innao, S. Russo, D. Gerace, A. Alonci, C. Musolino, Anticancer activity of curcumin and its analogues: preclinical and clinical studies, Cancer Invest. 35 (2017) 1–22;
(b) N.G. Vallianou, A. Evangelopoulos, N. Schizas, C. Kazazis, Potential anticancer properties and mechanisms of action of curcumin, Anticancer Res. 35 (2015) 645–652.
[29] P. Anand, A.B. Kunnumakkara, R.A. Newman, B.B. Aggarwal, Bioavailability of curcumin: problems and promises, Mol. Pharm. 4 (2007) 807–818.
[30] P. Anand, C. Sundaram, S. Jhurani, A.B. Kunnumakkara, B.B. Aggarwal, Curcumin and cancer: an "old-age disease with an "age-old" solution, Cancer Lett. 267 (2008) 133–164.
[31] P.S. Babu, K. Srinivasan, Influence of dietary curcumin and cholesterol on the progression of experimentally induced diabetes in albino rat, Mol. Cell. Biochem. 152 (1995) 13–21.
[32] P.S. Babu, K. Srinivasan, Hypolipidemic action af curcumin, the active principle of turmeric (Curcuma longa) in streptozotocin induced diabetic rats, Mol. Cell. Biochem. 166 (1997) 169–175.
33] C. Nirmala, R. Puvanakrishnan, Protective role of curcumin against isoproterenol induced myocardial infarction in rats, Mol. Cell. Biochem. 159 (1996) 85–93.
[34] C. Nirmala, R. Puvanakrishnan, Effect of curcumin on certain lysosomal hydrolases in isoproterenol-induced myocardial infarction in rats, Biochem. Pharmacol. 51 (1996) 47–51.
[35] K. Okada, C. Wangpoengtrakul, T. Tanaka, S. Toyokuni, K. Uchida, T. Osawa, Curcumin and especially tetrahydrocurcumin ameliorate oxidative stress-induced renal injury in mice, J. Nutr. 131 (2001) 2090–2095.
[36] N. Venkatesan, D. Punithavathi, V. Arumugam, Curcumin prevents adryamicin nephrotoxicity in rats, Br. J. Pharmacol. 129 (2000) 231–234.
37 (15)W.F. Chen, S.L. Deng, B. Zhou, L. Yang, Z.L. Liu, Curcumin and its analogues as potent inhibitors of low density lipoprotein oxidation: H-atom abstraction from the phenolic groups and possible involvement of the 4-hydroxy-3-methoxyphenyl groups, Free Radic. Biol. Med. 40 (2006) 526–535.
[38] J.S. Wright, Predicting the antioxidant activity of curcumin and curcuminoids, J. Mol. Struct. 591 (2002) 207–217.
[39] N. Venkatesan, M.N. Rao, Structure-activity relationships for the inhibition of lipid peroxidation and the scavenging of free radicals by synthetic symmetrical curcumin analogues, J. Pharm. Pharmacol. 52 (2000) 1123–1128.
[40] Y.M. Sun, H.Y. Zhang, D.Z. Chen, C.B. Liu, Theoretical elucidation on the antioxidant mechanism of curcumin: a DFT study, Org. Lett. 4 (2002) 2909–2911.
[41] K.I. Priyadarsini, D.K. Maity, G.H. Naik, M.S. Kumar, M.K. Unnikrishnan, J.G. Satav, Role of phenolic O-H and methylene hydrogen on the free radical reactions and antioxidant activity of curcumin, Free Radic. Biol. Med. 35 (2003) 475–484.
42A. Kunwar, K.I. Priyadarsini, Free radicals, oxidative stress and importance of antioxidants in human health, J. Med. Allied Sci.

1 (2011) 53–60.
[43] P. Anand et al, Biological activities of curcumin and its analogues (Congeners) made by man and Mother Nature, Biochem. Pharmacol. 76 (2008) 1590–1611.
[44] G. Czapski, S. Goldstein, Requirements for SOD mimics operating in vitro to work also in vivo, Free Radic. Res. Comm. 12–13 (1991) 167–171.
[45] J.S. Shim et al, Hydrazinocurcumin, a novel synthetic curcumin derivative, is a potent inhibitor of endothelial cell proliferation, Bioorg. Med. Chem. 10 (2002) 2987–2992.
[46] J.S. Shim, J. Lee, H.J. Park, S.J. Park, H.J. Kwon, A new curcumin derivative, HBC, interferes with the cell cycle progression on colon cancer cells via antagonization of the Ca2+/calmoduluin function, Chem. Biol. 11 (2004) 1455–1463.
[47] S. Dutta, S. Padhye, K.I. Priyadarsini, C. Newton, Antioxidant and antiproliferative activity of curcumin semicarbazone, Bioorg. Med. Chem. Lett. 15 (2005) 2738–2744.
[48] K. Mohammadi et al, Synthesis and characterization of dual function vanadyl, gallium and indium curcumin complexes for medicinal applications, J. Inorg. Biochem. 99 (2005) 2217–2225.
[49] A. Barik, B. Mishra, L. Shen, H. Mohan, R.M. Kadam, S. Dutta, H.-Y. Zhang, K.I. Priyadarsini, Evaluation of a new copper(II)-curcumin complex as superoxide dismutase mimic and its free radical reactions, Free Radic. Biol. Med. 39 (2005) 811–822.
[50] L. Baum, A. Ng, Curcumin interaction with copper and iron suggests one possible mechanism of action in Alzheimer's desease animal models, J. Alzh. Dis. 6 (2004) 367–377.
[51] O. Vajragupta, P. Boonchoong, H. Watanabe, M. Tohda, N. Kummasud, Y. Sumamont, Manganese complexes of curcumin and its derivatives: Evaluation for the radical scavenging ability and neuroprotective activity, Free Rad. Biol. Med. 35 (2003) 1632–1644.
[52] A. Barik, B. Mishra, A. Kunwar, R.M. Kadam, L. Shen, S. Dutta, S. Padhye, A.K. Satpati, H.-Y. Zhang, Priyadarsini, Comparative study of copper(II)-curcumin complexes as superoxide dismutase mimics and free radical scavenger, Eur. J. Med. Chem. 42 (2007) 431–439.
[53] J.P. Annaraj, K.M. Ponvel, P. Athappan, S. Srinivasan, Synthesis, spectra and redox behavior of copper(II) complexes of curcumin diketimines as models for blue copper proteins, Trans. Met. Chem. 29 (2004) 722–727.
[54] O. Vajragupta, P. Boonchoong, L. Berliner, Manganese complexes of curcumin analogues: evaluation of hydroxyl radical scavenging ability, superoxide dismutase ability and stability towards hydrolysis, Free Radic. Res. 38 (2004) 303–314.
[55] S. Banerjee, A.R. Chakravarty, Metal complexes of curcumin for cellular imaging, targeting, and photoinduced anticancer activity, Acc. Chem. Res. 48 (2015) 2075–2083.
[56] T. Sarkar, S. Banerjee, S. Mukherjee, A. Hussain, Mitochondrial selectivity and remarkable photocytotoxicity of a ferrocenyl neodymium(III) complex of terpyridine and curcumin in cancer cells, Dalton Trans. 45 (2016) 6424–6438.
[57] A. Garai, I. Pant, S. Banerjee, B. Banik, P. Kondaiah, A.R. Chakravarty, Photorelease and cellular delivery of mitocurcumin from its cytotoxic cobalt(III) complex in visible light, Inorg. Chem. 55 (2016) 6027–6035.

[58] S. Banerjee, I. Pant, I. Khan, P. Prasad, A. Hussain, P. Kondaiah, A.R. Chakravarty, Remarkable enhancement in photocytotoxicity and hydrolytic stability of curcumin on binding to an oxovanadium(IV) moiety, Dalton Trans. 44 (2015) 4108–4122.
[59] K. Mitra, S. Gautam, P. Kondaiah, A.R. Chakravarty, Platinum(II) complexes of curcumin showing photocytotoxicity in visible light, Eur. J. Inorg. Chem. 1753– 1763 (2017).
[60] T. Sarkar, A. Hussain, Photocytotoxicity of curcumin and its iron complex, Enz. Eng. 5 (2016), https://doi.org/10.4172/2329-6674.1000143.
[61] U. Bhattacharyya, B. Kumar, A. Garai, A. Bhattacharyya, A. Kumar, S. Banerjee, P. Kondaiah, A.R. Chakravarty, Curcumin "Drug" stabilized in oxidovanadium(IV)-BODIPY conjugates for mitochondria-targeted photocytotoxicity, Inorg. Chem. 56 (2017) 12457–12468.
[62] B. Deka, S. Mukherjee, A. Bhattacharyya, T. Sarkar, K. Soni, S. Banerjee, K.K. Saikia, S. Deka, A. Hussain, Ferrocene conjugated copper(II) complexes of terpyridine and traditional Chinese medicine (TCM) anticancer ligands showing selective toxicity towards cancer cells: Ferrocenyl copper(II) complexes of traditional Chinese Medicines, Appl. Organometal. Chem. 32 (2018), https://doi.org/10.1002/aoc.4287 e4287.
[63] C.Gh. Macarovici, Quantitative Inorganic Chemical Analysis, Ed. Acad. RSR, Bucharest, 1979.
[64] W.A. Boggust, W. Cocker, Experiments in the chemistry of benzothiazole, J. Chem. Soc. 355–362 (1949).
[65] E. Jo´ na, L. Lajdova´ , L. Kvasnicova´ , S. Lendvayova´, M. Pajta´ s˘ova´ , D. Ondrus˘ova´ , P. Liza´ c, S.C. Mojumdar, Thermal properties of solid complexes with biologically important heterocyclic ligands. Part III. Thermal decomposition and infrared spectra of thiocyanato Mg(II) complexes with 2- hydroxypyridine, quinoline, and quinoxaline, J. Therm. Anal. Calorim. 104 (2011) 817–821.
[66] I.A. Tossidis, C.A. Bolos, A. Christofides, Monohalogenobenzoylhydrazones VI. New antimony(III) complexes with monochlorobenzoylhydrazones of 2- furaldehyde, 2-pyrrolaldehyde and 2-thiophenaldehyde as ligands, J. Therm. Anal. 35 (1989) 1339–1350.
[67] J. Bao, C. Tang, R. Tang, Synthesis and luminescent properties of novel pyrazolone rare earth complexes, J. Rare Earths 29 (2011) 15–19.
[68] H.F. Abd El-Halim, F.A. Nour El-Dien, G.G. Mohamed, N.A.mMohamed, Synthesis,, spectroscopic, thermal characterization and antimicrobial activity of miconazole drug and its metal complexes, J. Therm. Anal. Calorim. 109 (2012) 883–892.
[69] M. Ca˘ linescu, D. Manea, G. Pavelescu, Synthesis and spectroscopic properties of new complex compounds of europium(III) and terbium(III) with 2-hydroxy-1- naphthaldehyde acetylhydrazone and heterocyclic bases, Rev. Roum. Chim. 56 (2011) 231–237.
[70] C. Vansant, H.O. Desseyn, S.P. Perlepes, The synthesis, spectroscopic and thermal study of oxamic acid compounds of some metal(II) ions, Transition Met. Chem. 20 (1995) 454–459.
[71] M. Ca˘ linescu, E. Ion, A.-M. Stadler, Studies on nickel(II) complex compounds with 2-benzothiazolyl hydrazones, Rev. Roum. Chim. 53 (2008) 903–909.
[72] M.A. Subhan, K. Alam, M.S. Rahaman, M.A. Rahman, M.R. Awal, Synthesis and characterization of metal complexes containing curcumin (C21H2O6) and study on their antimicrobial activities on DNA binding properties, J. Sci. Res. 6 2014) 97–109.
[73] S. Dutta, A. Murugkar, N. Gandhe, S. Padhye, Enhanced antioxidant activities of metal conjugates of curcumin derivatives, Met. Based Drugs 8 (2001) 183–188.
[74] A.P. Zambre, V.M. Kulkarni, S. Padhye, S.K. Sandur, B.B. Aggarwal, Novel curcumin analogs targeting TNF-induced NFjB activation and proliferation in human leukemic KBM-5 cells, Bioorg. Med. Chem. 14 (2006) 7196–7204.
[75] E.B. Seena, M.R. Prathapachandra Kurup, Spectral and structural studies of mono- and binuclear copper(II) complexes of salicylaldehyde N(4)-substituted thiosemicarbazones, Polyhedron 26 (2007) 829–836.
[76] R.L. Dutta, Md.M. Hossain, Coordination chemistry of acyl, aroyl, heteroaroyl hydrazones and related ligands, J. Sci. Ind. Res. 44 (1985) 635–674.
[77] A.B.P. Lever, Inorganic Electronic Spectroscopy, second ed., Elsevier, Amsterdam-Oxford-New York-Tokyo, 1984.
[78] R. Re, N. Pellegrini, A. Pannala, M. Yang, C. Rice-Evans, Antioxidant activity applying an improved ABTS radical cation decolorization assay, Free Radical. Biol. Med. 26 (1999) 1231– 1237.